Journals Pub

International Journal of
Mechanics and Design

ISSN: 2582-2896
Volume 11, Issue 1, 2025
January—June
DOI (Journal): 10.37628/IJMD

https://journalspub.com/journal/ijmd/

Research IJMD

Experimental Investigation on Cylindrical Mid-Section with Different Forebody Profiles

Kush Kumar*

Abstract

In this work, the experimental approach was used to study the aerodynamic performance of cylindrical mid-section with various forebody profiles. The aerodynamic characteristics, such as static pressure, axial velocity, and coefficient of pressure for cylindrical mid-section with various forebody profiles were investigated for subsonic speed for the same length-to-diameter ratio. The experimental work was conducted at a flow velocity of approximately 25 m/s and calculations were done for zero degrees angle of attack to demonstrate the flow behavior. The experimental data of each test was compared to find out the deviation between static pressure, and axial velocity. From the study, it is concluded that the sharp tip forebody profiles have a small stagnation region over the cylindrical mid-section and the blunted tip of the forebody has a bigger stagnation region over the cylindrical mid-section, therefore the aerodynamic properties vary over the cylindrical mid-section-due to the shape of various forebody profiles. Thus, the cylindrical mid-section with power series 1.0 forebody reaches greater velocities with low static pressure from leading to the trailing edge.

Keywords: Forebody, aerodynamic performance, cylinder, wind tunnel, Static Pressure Deviation

INTRODUCTION

When rockets and missiles are in flight, many forces act on the surface of the body, such as lift and drag. During the course, flight vehicles experience two types of drag namely Wave Drag and Skin Friction Drag which the speed of the vehicle may be vehicle reduced. Maintaining a level flight for a vehicle requires a greater quantity of fuel, so the weight of the vehicle also increases [1]. Therefore, during the design of the vehicle, the major goal is minimizing the drag on each part of the vehicle.

The vehicle consists of three parts:

- Forebody.
- Mid-Section.
- Tail-Section.

Forebody

Forebody has a major effect on the performance of the vehicle. The selection of the forebody depends on the mission requirement and minimum drag condition to maximize the lift. Drag depends on many factors, such as the shape of the body, fluid characteristics, and orientation of the body in fluid. That is why many different shapes of forebody are utilized in modern vehicles [2] one of which can be seen in Figure 1.

where,
L = Overall length of forebody.
R = the radius of the base of the forebody.
y = radius at any point x.

***Author for Correspondence**
Kush Kumar
E-mail: chauhankushkumar@gmail.com

Research Scholar, Aerospace Engineering Department, Amity University, Gurgaon, Haryana, India

Received Date: February 12, 2025
Accepted Date: February 14, 2025
Published Date: March 28, 2025

Citation: Kush Kumar. Experimental Investigation on Cylindrical Mid-Section with Different Forebody Profiles. International Journal of Mechanics and Design. 2025; 11(1): 44–53p.

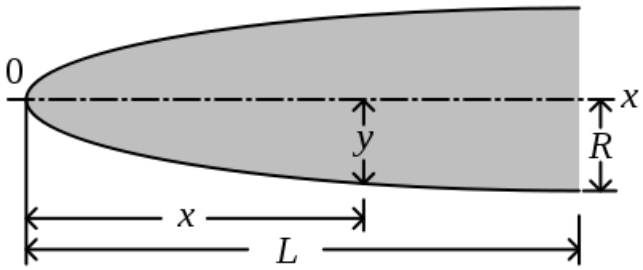

Figure 1. General shape of forebody [2].

Mid-Section

The main purpose of the mid-section is to store the maximum amount of payload in a small area. The mid-section is mostly used in the circular cylinder body (Figure 2) because the flow separation occurs from 80 to 90 degrees over the smooth cylinder body on either side of the cylinder from the upstream stagnation point. The lift-to-drag ratio is maximum at 45 degrees and the minimum condition at 75 degrees on the cylinder body [3–4].

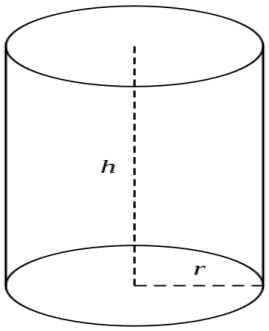

Figure 2. Cylinder body [3].

BACKGROUND STUDY

The flow around the circular cylinder has various regions, such as critical, sub-critical, and super-critical regions that occur due to stagnation region and higher static pressure over the surface of the circular body. Many studies have been conducted on the study of flow properties over the circular cylinder by Karman. Karman studied the vortex street around the circular cylinder body. The researcher studied flow separation on a cylinder body in the ground using experimental and numerical methods. In, addition, unsteady flow research is useful in rocket launches, turbo machinery, flutter, dynamic stall, and vehicles on the ground. Prandtl was the first to research accelerated unsteady flow by visualization of initial vortex formation over a circular cylinder [5–6]. Summer and Fredsoe [7] observed the flow around a circular cylinder. The flow filed around the cylinder was symmetric at Re < 2000. This study also focused on the variation of Reynolds number. As the Reynolds number increases then the flow begins to separate behind the cylinder. Due to the separation of flow, vortex shedding also takes place. Park et al. [8] studied the flow properties over the circular cylinder with a low Reynolds number. Zdravkovich [9] numerically and experimentally studied the flow properties around the bluff bodies and defined the transition region of flow from laminar to turbulent. Young and Ooi [10] studied the impact of variation in inlet turbulence length with Re $1.4x10^5$ by using the SST k-w model. Oudheusden et al. [11] performed an experimental study on the vortex formation and shedding closer to the wake region around the square cylinder with Re 2×10^4. Benim [12] investigated the numerical study on turbulence flow over the circular cylinder by using the SST k-w model with Re from $1x10^4$ and $5x10^6$. This study focused on the critical flow regions. Holzer and Sommerfeld [13] computed the drag coefficient by using the SST k-w model. This study found that the drag coefficient is low at a low Reynolds number. Gao and Tamura [14] compared the experimental and numerical study of aerodynamic forces and vortex shedding around the circular cylinder with Re from 1×10^4 and 6×10^5. Rajani et al. [15] studied the numerical study of laminar flow over circular cylinders for Re 1×10^5 to

4 x 10^5. Ong [16] studied the 2-D unsteady flow properties around the circular cylinder with Re 1 x 10^6 and 2 x 10^6. In this study, Navier-Stokes equation was utilized. Bai and Li [17] studied the hydrodynamic properties of flow over the circular cylinder in 2-D unsteady flow by using CFD software within Reynolds number 2 x 10^6. This study investigated the pressure distribution, drag, and lift coefficient. Kozlov [18] investigated the 2-D flow past a circular cylinder within range of Reynolds number from 5 x 10^5 to 2 x 10^6. In this study, A Fourier transformer algorithm was used to solve the Poisson equation in rectangular meshes with complex geometries. Butt and Egbers [19] studied the drag characteristics of flow over the circular cylinder. The large drag occurs on the surface of the body due to a major difference in pressure between the upstream and downstream. From this effect, the flow separation generates alternatively over the surface of the cylinder.

EXPERIMENTAL SETUP

Wind Tunnel Calibration

The main objective of wind tunnel calibration is to find out the point of least fluctuation in velocity during different trials. Velocity calibration is required to compute the actual velocity of airflow in the test section. The rpm of the motor was varied from 30–50 variances. The least amount of fluctuation was found at 50 variances of the motor. Tables 1 and 2 show the two trials for the calibration of the wind tunnel.

Table 1. Inlet velocity calibration (experimental).

H_1 (cm)	H_2 (cm)	Δ H (m)	V (m/s)
11.1	24.5	0.039858	24.46691
11.3	24.4	0.039858	24.80209
11.2	24.6	0.39858	25.378
11.3	24.4	.040117	25.29653
11.3	24.5	0.039858	25.05053

Note: The average velocity of this trial = 24.998812 m/s.

Table 2. Inlet velocity calibration (experimental).

H_1 (cm)	**H_2 (cm)**	**Δ H (m)**	**V (m/s)**
10.5	25.1	0.037788	24.55113
10.6	25	0.03727	24.38239
10.4	25.4	0.038823	24.88517
10.3	25.6	0.039599	25.13279
10.2	25.8	0.040376	25.378

Note: The average speed of this trial = 24.9.

Validation for Experimental Setup

Before performing experimental analysis on wind tunnel, validation is required to find the actual percentage error in experimental and theoretical data. For the validation of the experimental setup, the cylindrical profile has been taken as the test object. The dimension of the cylindrical profile was (300 x50mm). The data of this profile has been taken at different angles at the same velocity.

The velocity calculation has been done by expression as shown in Equation 1.

$$C_P = 1 - (v/ v_\infty)^2 \quad (1)$$

Rearranging the above equation,

$$V = V_\infty (1 - C_P)^{0.5} \quad (2)$$

The theoretical value of the coefficient of pressure for the cylinder profile has been calculated from Equation 3.

$$C_P = 1 - 4\sin^2 \alpha \quad (3)$$

Table 3 shows the calculated *Cp* experimental values while Table 4 shows the difference between the theoretical and experimental values of *Cp*.

Table 3. *Cp* Experimental.

h1 (cm)	h2 (cm)	(h2–h1) (m)	A	C_p Experimental
0.0	4	0.040	0	1
0.3	4	0.037	10	0.925
1.7	4	0.023	20	0.575
3.4	4	0.006	30	0.150
6.3	4	–0.023	40	–0.575
9.0	4	–0.050	50	–1.250
11.3	4	–0.073	60	–1.825

Table 4. Difference between Cp (theoretical) and Cp (experimental).

C_p Experimental	C_p theoretical	Error
1.000	1.000	0.0
0.925	0.879	4.5
0.575	0.532	4.2
0.060	0.000	6.0
–0.575	–0.652	7.7
–1.250	–1.347	9.7
–1.925	–2.000	7.5

Figure 3 shows the comparative plot of experimental and theoretical values of C_p.

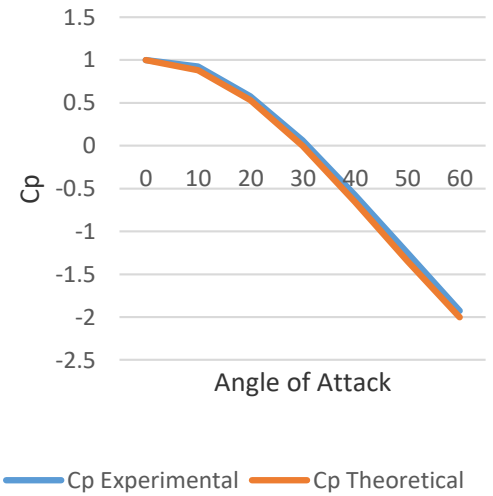

Figure 3. Comparison of Cp (theoretical) and Cp (experimental).

Model Setup in Wind Tunnel

The length of the nosecone is 117 mm, and the diameter is 79 mm. The length of the body section (cylindrical body as mid-section) is 200 mm, and the diameter is 79 mm. A total of 10 holes are punched on the surface of the mid-section along the length, where the properties of flow have been determined. Many tests have been done for different types of nosecone with cylindrical mid-section at a velocity of 25 m/s.

Figure 4 shows the cylindrical mid-section with 10 holes. Figures 5, 6, and 7 show the different configurations of power series nose cones selected for the experimental tests.

Table 5. Distance of static ports over cylinder mid-section.

S.N.	Static Port No.	Distance (mm)
1.	P1	11
2.	P2	31
3.	P3	51
4.	P4	91
5.	P5	71
6.	P6	111
7.	P7	131
8.	P8	151
9.	P9	171
10.	P10	191

Figure 4. Cylindrical mid-section body with 10 holes.

Figure 5. Experimental setup of cylindrical mid-section with power series1 forebody.

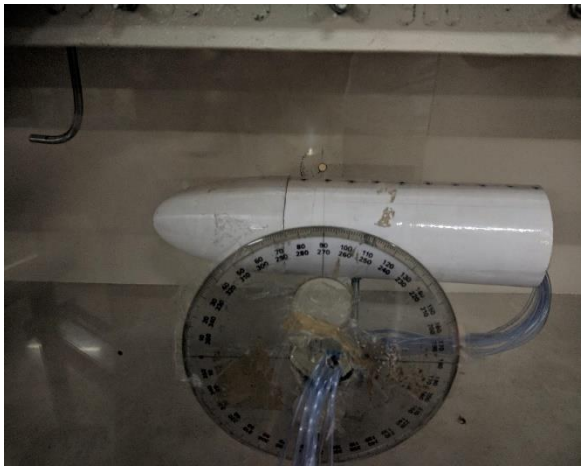

Figure 6. Experimental setup of cylindrical mid-section with power series 0.25 forebody.

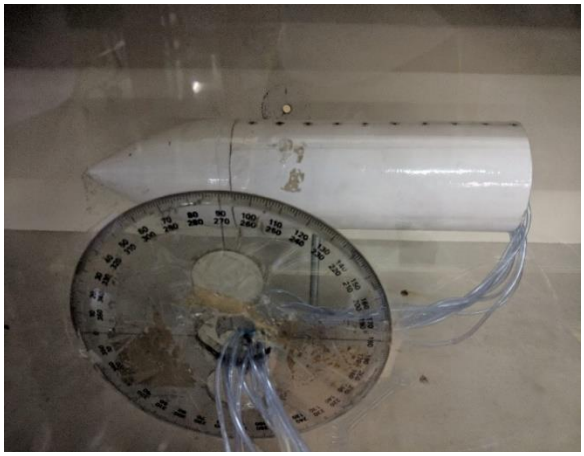

Figure 7. Experimental setup of cylindrical mid-section with secant ogive forebody.

RESULT AND DISCUSSION

Comparison of Static Pressure for Cylindrical Mid-Section with Various Forebody

Figure 8 shows that the cylindrical mid-section with power series 1.0 forebody has the least static pressure over the surface. This is because the power series 1.0 configuration makes a small, wet area with airflow leading to a small stagnation region and the suction of flow decreases over the length of the mid-section. The cylindrical mid-section with power series 0.25 has maximum static pressure because this configuration makes a higher wet area in the flow filed and hence the stagnation region is bigger over the surface of the cylindrical body as compared to configurations.

Comparison of Velocity for Cylindrical Mid-Section with Various Forebody

The velocity is inversely proportional to the pressure so, the power series 1.0 forebody with cylindrical mid-section reaches higher velocities when compared to other profiles because this forebody has a sharp tip which produces a smaller stagnation region and low static pressure leading to the trailing edge of cylindrical mid-section (Figure 9). This is the reason for the higher velocity of flow over the surface. But the configuration of power series 0.25 forebody profile with cylindrical mid-section reaches lower velocities because this forebody has a blunted shape at the tip and the stagnation region is bigger, therefore the static pressure is also higher, and the dynamic pressure is low.

Comparison of Coefficient of Pressure for Cylindrical Mid-Section with Various Forebody Profiles

Every point has a unique value of C_P in the flow field. From Figure 10, it can be seen that the magnitude of C_P decreases with increases in the distance of the static port over the surface of the cylinder

because the suction of flow decreases and the potential energy of flow converts into kinetic energy which the velocity of flow increases and the ratio of local pressure to dynamic pressure over the length of cylindrical mid-section decreases. C_P is inversely proportional to the square of velocity at any point in each time.

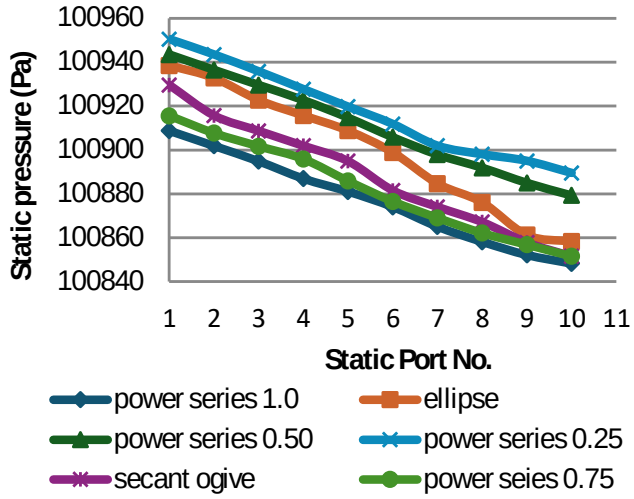

Figure 8. Comparison of static pressure for cylindrical mid-section with various forebody.

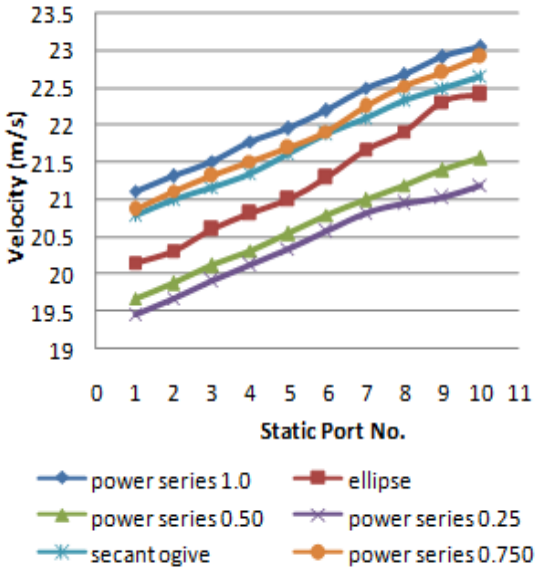

Figure 9. Comparison of velocity for cylindrical mid-section with various forebody.

Comparison of Velocity Deviation for Cylindrical Mid-Section with Various Forebody

The velocity deviation represents the flow pattern over the surface of the body. If the deviation is zero, then flow moves over the body with the same velocity and pattern. If the deviation is higher then flow moves over the body with a less uniform pattern and when the deviation is small, then the flow moves with a more uniform pattern. From Figure 11, it is evident that the cylindrical mid-section with power series 1.0 has a low deviation in velocity from the average velocity. The flow may move over the surface of the body with a uniform pattern. The cylindrical mid-section with an ellipse forebody has a higher deviation, so the flow pattern changes rapidly.

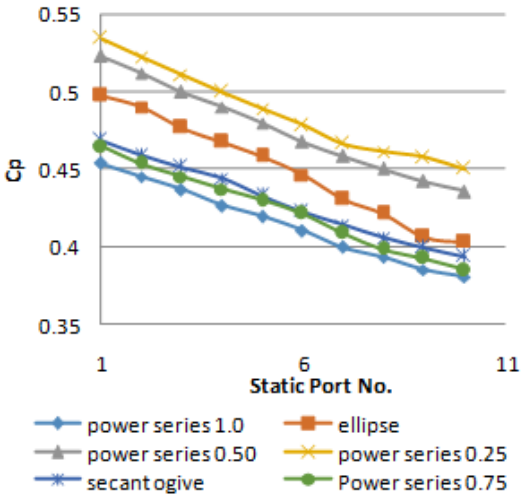

Figure 10. Comparison of coefficient of pressure for cylindrical mid-section with various forebody.

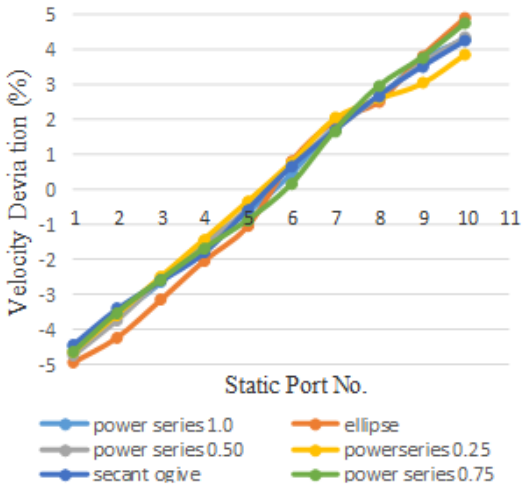

Figure 11. Comparison of velocity deviation for cylindrical mid-section with various forebody.

Comparison of Static Pressure Deviation for Cylindrical Mid-Section with Various Forebody

The static pressure deviation represents the flow pattern over the surface of the body. If the deviation is zero, then the flow moves over the body with the same pressure magnitude and pattern. If the deviation is higher then flow moves over the body with a less uniform pattern and when the deviation is small, then the flow moves with a more uniform pattern. From Figure 12, the cylindrical mid-section with power series 1 has a small deviation because this profile has a small stagnation region leading to the trailing edge of the cylindrical mid-section body due to the sharp edge of the forebody with small curvature which the variation in static pressure is very low.

CONCLUSIONS

In this work, the experimental approach was used to study the aerodynamic performance of cylindrical mid-sections with various forebody profiles, such as static pressure, coefficient of pressure, axial velocity, etc. of cylindrical mid-section with the various forebody profiles.

The experimental analysis was obtained for subsonic conditions for profiles of the same length-to-diameter ratio. The study involves a velocity of 25 m/s and the other parameters were measured and calculated for zero angle of attack and then compared to each other.

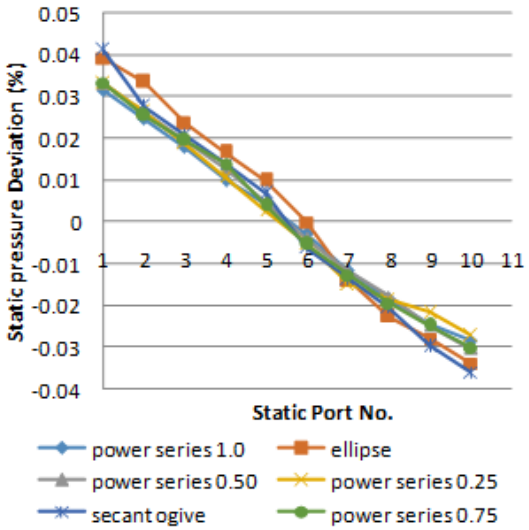

Figure 12. Comparison of static pressure for cylindrical mid-section with various forebody.

From this study, it this found that the cylindrical mid-section with power series 1.0 reaches higher velocity with low static pressure and small deviation in velocity and static pressure.

REFERENCES

1. Ranjan GRR, Parmar DV, Raipuria HK, Singh PB. Innovative forebody design of aircraft. In: ASME International Mechanical Engineering Congress and Exposition. Vol. 1. 2015.
2. Chinn SS. Missile configuration design. New York: McGraw-Hill Book Co., Inc.; 1961.
3. Mallick M, Kumar A. Study on drag coefficient for the flow past a cylinder. National Institute of Technology. 201;5(4):301–306.
4. Abide S, Viazzo S. A 2-D compact fourth-order projection decomposition method. J Comput Phys. 2005;206(1):252.
5. Takayama S, Aoki K. Flow characteristics around a rotating grooved circular cylinder with grooves of different depths. J Vis. 2005;8(4):295–303.
6. Gera B, Sharma PK, Singh RK. CFD analysis of 2D unsteady flow around a square cylinder. Int J Appl Eng Res. 2010;1(3):602.
7. Sumer BM, Fredsøe J. Hydrodynamics around cylindrical structures. Advanced Series on Ocean Engineering. Vol. 12. Singapore: World Scientific; 1997.
8. Park J, Kwon K, Choi H. Numerical solution of flow past a circular cylinder at Reynolds numbers up to 160. KSME Int J. 1998;12(6):1200.
9. Zdravkovich MM. Flow around circular cylinders: fundamentals. Vol. 2. New York: Oxford University Press; 2003.
10. Young ME, Ooi A. Turbulence models and boundary conditions for bluff body flow. In: Proceedings of the 15th Australasian Fluid Mechanics Conference; Sydney, Australia; 2004.
11. Oudheusden BWV, Scarano F, Hinsberg NPV, Watt DW. Phase-resolved characterization of vortex shedding in the near wake of a square-section cylinder at incidence. Exp Fluids. 2005;39(1):86.
12. Benim AC, Cagan M, Nahavandi A, Pasqualotto E. RANS predictions of turbulent flow past a circular cylinder over the critical regime. In: Proceedings of the 5th IASME/WSEAS International Conference on Fluid Mechanics and Aerodynamics; Athens, Greece; 2007.
13. Hölzer A, Sommerfeld M. New simple correlation formula for the drag coefficient of non-spherical particles. Powder Technol. 2008;184(3):361.
14. Cao S, Tamura Y. Flow around a circular cylinder in linear shear flows at subcritical Reynolds number. J Wind Eng Ind Aerodyn. 2008;96(10–11):1961.
15. Rajani BN, Kandasamy A, Majumdar S. Numerical simulation of laminar flow past a circular cylinder. Appl Math Model. 2009;33(3):1228–1247

16. Ong MC, Utnes T, Holmedal LE, Myrhaug D, Pettersen B. Numerical simulation of flow around a smooth circular cylinder at very high Reynolds numbers. Mar Struct. 2009;22:142.
17. Bai H, Li JW. Numerical simulation of flow over a circular cylinder at low Reynolds number. Adv Mater Res. 2011;255–260:942.
18. Kozlov IM, Dobergo KV, Gnesdilov N. Application of RES methods for computation of hydrodynamic flows by an example of 2D flow past a circular cylinder for Re = 5–200. Int J Heat Mass Transf. 2011;54(4):887.
19. Butt U, Egbers C. Aerodynamic characteristics of flow over circular cylinders with patterned surface. Int J Mater Mech Manuf. 2013;1(2):121.

Nomenclature

A_{wet}	Wetted area
C_p	Coefficient of pressure
C_{fx}	Skin -friction drag coefficient for laminar flow
C_{fT}	The skin-friction drag coefficient for turbulent flow
C_f	Skin –friction drag for the whole body
C_D	Coefficient of drag
C_{Di}	Induced drag
C_L	Lift coefficient
D	Diameter of nose cone at body joint
E	Bulk modulus elasticity
g	Acceleration due to gravity
h	Length of mid-section
ΔH	Pressure head
P	Power of nose cone
p	Density of fluid
p_w	Density of water
p_a	Density of air
P_∞	Free stream Pressure
R	The radius of nose cone

